

RESEARCH

Open Access



Development of craquelure patterns in paintings on canvas

Marcin Bury¹ and Łukasz Bratasz^{1*}

Abstract

Canvas paintings are layered structures composed of canvas support sized with animal glue, a preparatory layer of the ground, and paint and varnish layers on the top. Preventing or limiting humidity-induced stresses in these structures requires an understanding of the relevant processes and risks. A three-dimensional model of a canvas painting was used to analyse stresses and crack development in the two-layer structure comprised of a glue-sized canvas on a wooden stretcher with a layer of stiff chalk-glue ground representing a pictorial layer in historic canvas paintings. The model was subjected to a large relative humidity fall which induced shrinkage of the glue-sized canvas. The modelling revealed that when a stretcher with flexible wooden bars is considered, high tensile stresses arise in the ground layer at the corners of the painting, and cracks are formed in these areas in the direction perpendicular to the painting's diagonal. Ratios of critical distances between cracks to the ground layer thickness for which stresses in the midpoints between the cracks dropped to below the level inducing fracture in the material were estimated for various magnitudes of the relative humidity drop and thicknesses of the ground layer. Increasing ground layer thickness limits the hygric response of the sized canvas and makes the paintings less vulnerable to humidity variations. The ratio of stress along the diagonal calculated for painting with one crack to the solution without cracks was described by the double Lorentz function. A simple procedure of calculating stress variations along the diagonal—using the function—on a sequential addition of cracks was developed. Cracks in central parts of canvas painting were found to be induced by permanent cumulative drying shrinkage of the oil-based paints and grounds due to the evolution of the molecular composition of the oil binder. The outcome of the modelling indicated that the risk of cracking of the pictorial layers in canvas paintings due to drops in ambient relative humidity was small.

Keywords Canvas paintings, Numerical modelling, Crack formation, Craquelure patterns, Fracture saturation, Indoor climate, Collection care

Introduction

Cracks in paintings are formed due to drying and chemical evolution of paints or grounds, instabilities in the painting's environment, excessive stretching of the canvas support, and mechanical impacts during handling. Craquelure patterns are related to the materials and painting techniques employed by artists and are an

important element in judging the authenticity of the work. The craquelure on a painting changes its visual appearance. While the craquelure is generally perceived as a natural alteration that may enrich the viewer's perception, environmental and physical impacts may lead to the formation of new disfiguring cracks and the progressing deterioration of painted surfaces that requires improvements in the collection care to prevent permanent loss of artistic quality and authentic material. Therefore, various aspects of crack formation and propagation have been studied in the past.

*Correspondence:

Łukasz Bratasz
lukasz.bratasz@ikifp.edu.pl

¹ Jerzy Haber Institute of Catalysis and Surface Chemistry Polish Academy of Sciences, 30-239 Kraków, Poland



© The Author(s) 2024. **Open Access** This article is licensed under a Creative Commons Attribution 4.0 International License, which permits use, sharing, adaptation, distribution and reproduction in any medium or format, as long as you give appropriate credit to the original author(s) and the source, provide a link to the Creative Commons licence, and indicate if changes were made. The images or other third party material in this article are included in the article's Creative Commons licence, unless indicated otherwise in a credit line to the material. If material is not included in the article's Creative Commons licence and your intended use is not permitted by statutory regulation or exceeds the permitted use, you will need to obtain permission directly from the copyright holder. To view a copy of this licence, visit <http://creativecommons.org/licenses/by/4.0/>. The Creative Commons Public Domain Dedication waiver (<http://creativecommons.org/publicdomain/zero/1.0/>) applies to the data made available in this article, unless otherwise stated in a credit line to the data.

Attempts to classify and characterize cracks were made by Stout [1] and Bucklow [2]. Bucklow showed that there were distinct variations in craquelure patterns between different chronological and geographical artistic traditions, including materials and their application. Two primary mechanisms of crack formation and corresponding types of crack patterns were distinguished: drying and ageing cracks. Drying cracks are induced by the shrinkage of drying materials contained in the pictorial layer, restrained by the dimensionally stable substrates. The drying shrinkage is a cumulative process related to the gradual loss of water from glue-based grounds or tempera paints [3, 4] or the evolution of the molecular composition of the oil binder in paints or grounds, especially the evaporation of low-molecular-weight organic components [5, 6]. Both processes lead to the development of voids locked in the materials. Over time, their densification is observed—voids diffuse out—and pigment particles are held together more tightly by the binder lattice. In turn, ageing cracks are engendered by humidity-induced cyclic swelling or shrinkage of the wood or canvas substrate [7, 8]. Both cracking mechanisms are explained by the stress transfer from the substrate to the uncracked layer or—if cracks are already present—to the area between neighbouring cracks. Stress reaches its maximum value in the middle of the crack-free area [9]. If stress exceeds the strength of the material, a new crack nucleates. Ultimately, the crack saturation occurs and an additional load does not initiate new fractures [10, 11]. The craquelure patterns in paintings were investigated in recent publications [12, 13] and thoroughly reviewed by Pauchard and Giorgiutti-Dauphiné [14].

Paintings on canvas are layered structures composed of canvas support sized with animal glue, a preparatory layer of the ground, and paint and varnish layers on the top. Further, paintings may comprise materials added in conservation treatments to reinforce the painted structure. In 1982, Mecklenburg introduced a laminar structural model for canvas paintings assuming that the overall structural response of a painting could be determined by the superposition of individual responses of all its components [15]. The laminar model has been further refined by considering glue-sized canvas or canvas lined with wax-resin adhesive to be composite substrates showing specific composite performance [8, 16, 17]. The model pinpointed two humidity conditions leading to substantial forces within the layered structure of paintings when subjected to changes in relative humidity (RH). At low RH levels, the glue size undergoes shrinkage generating high stress when constrained. Generally, forces developed in restrained and desiccated oil paints and ground are notably lower than those in the

canvas and glue size. This difference has been attributed to the ground containing a significant volume fraction of non-adsorbing filler and often featuring oil as a binder. In turn, the painting dimensional response at high RH levels depends on the textile structure and material characteristics of the adhesive. Janas et al. established that swelling of glue sizing dominated the moisture-induced dimensional expansion of the canvas-glue composite in the less stiff direction in the textile, completely overriding the shrinkage of the untreated canvas [8]. In turn, embedding the fibres of the canvases in wax resin in the course of lining caused not only a notable shrinkage of the composite at high RH levels but also shifted the onset of shrinkage to a low RH level of approximately 60–65% compared to the unlined sample [17]. The model's predictions aligned well with the observed force development in actual paintings, providing insight into damage mechanisms such as tenting and flaking of the pictorial layer due to canvas shrinkage.

The laminar model of canvas paintings was supported and refined by computer-aided simulations. As presented in Lee et al. [18], Mecklenburg and Tumosa employed the finite element model (FEM) to evaluate stress levels and distributions in oil paintings on canvas exposed to varying temperature and RH [19]. The models consisted of flat sheets of canvas, glue, and paint layers in full contact with each other and restrained on the circumferential edges of the canvas. The research revealed stress concentrations near painting corners and variations in stress directions across different areas, mirroring crack patterns seen in historical paintings [20]. Similar modelling of oil canvas paintings by de Willigen produced comparable results [21]. Lee et al. further refined the laminar model by replacing fixed edge boundary conditions with a realistic geometrical deformation of the stretcher bars [18]. Moreover, the authors used a combination of FEM and extended finite element method (XFEM) to approximate and understand the underlying mechanisms of crack initiation and propagation at the local scale. Several combinations of canvas, animal glue sizing, two grounds, and two oil paints were analysed. The results of the simulations showed that the shrinkage of the glue induced the deformation of the stretcher—the middle parts of the stretcher bars were pulled towards the painting's centre. This deformation was the primary source of the tension reduction in the centre of the painting. The authors determined the critical value of RH drop that caused crack initiation to be 48% for the worst-case combination of sizing, ground, and paint.

This paper reports on the FEM modelling of the crack pattern development in the two-layer structure of the canvas painting—the glue-sized canvas and the chalk-glue

ground—experiencing stress induced by glue shrinkage under the desiccation of the painting. Differently to Lee et al. [18], the glue-sized canvas was considered in the modelling as a composite rather than composed of two distinct layers, the properties and performance of the composite being affected both by the textile structure and material characteristics of the glue [8]. In turn, the chalk-glue ground was selected to represent a pictorial layer. Though oil grounds predominate in canvas paintings, chalk-glue grounds were popular among painters and are described in many historical recipes, also as a first layer followed by a second oil-bound layer [22, 23]. Moreover, oil-based pictorial layers are known to evolve for years, even centuries. Therefore, mechanical properties available for oil-based paints naturally aged for a limited time would not mimic old historic paintings. In consequence, the chalk-glue ground has been indicated as having mechanical properties close to old brittle oil-based materials which can be used as substitutes for the historic pictorial layers [24, 25].

A three-dimensional fully elastic model was used to analyse the distribution of principal stress components in the pictorial layer and, in this way, to understand how cracks are formed in the painting's corners under desiccation and what is their impact on the vulnerability of the painting to environmental variations. In particular, ratios of distances between the corner cracks to the ground layer thickness were estimated for increasing shrinkage of the glue-sized canvas. The model predictions, the average crack distance as well as the surface of cracked areas, are compared with crack patterns in a mock-up painting exposed to RH variations in an environmental chamber.

Methods

Model

The model of a canvas painting consisted of a bilayer structure—sized canvas covered with a ground—stretched on a wooden stretcher. The FE method was used to perform analysis under the assumption of fully elastic properties of all materials. COMSOL Multiphysics software Version 6.0 from COMSOL AB (Stockholm) with coupled solid mechanics and heat transfer modules was used to compute static solutions of deformation problems for a painting, induced by humidity variations. Two geometries of the model were considered: one of an uncracked painting to analyse stress distribution and establish positions of cracks, the other of a painting with cracks introduced into the ground layer. The aspect ratio of the stretcher bars is one of the properties that affect how the displacements are distributed in the model. There has been a multitude of painting sizes and aspect ratios used by painters. In this study, dimensions used in

the earlier modelling study of Lee et al. were chosen, that is to say, dimensions typical of the 19th-century Danish Golden Age paintings with the height-to-width ratio of 1:1.2 and a total size of 635 by 762 mm [18].

It was assumed that the bars of the stretcher were made of wood cut in the longitudinal direction and their width and thickness in the radial and tangential directions were 40 and 20 mm, respectively. The ends of the wood pieces were cut at a 45-degree angle to adhere to the corners. Further, small protruding wooden elements (profiles) 10 mm wide and 5 mm thick were adhered to the bars providing the support of the canvas to the stretcher (Fig. 1).

Earlier research has revealed stress concentrations near painting corners with the maximum stresses close to the diagonal of the painting leading to the formation of cracks in the direction perpendicular to the diagonal. To study the impact of such cracks on the stress field, four parallel cracks spanning between the edges of the wooden profiles of the stretcher were introduced as discontinuities penetrating the entire thickness of the ground layer in the direction perpendicular to the painting's diagonal (Fig. 2). First, the stress plot along the diagonal was established and the first crack was located in the area of the highest stresses next to the painting's edges. Further, one crack towards the painting's corner and two cracks towards the painting's centre were added. Each crack was represented as a single boundary across which the displacement field was discontinuous. Stress relaxation came from crack widening only, and the model did not simulate the propagation of cracks. The distance between all cracks S was the same and it was a free parameter in the study.

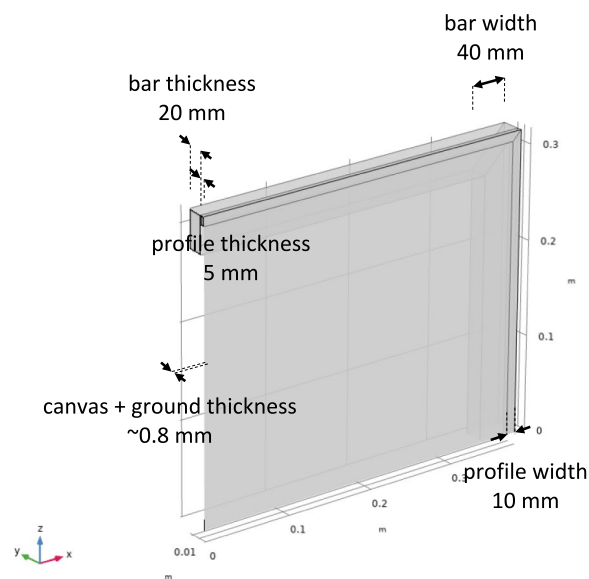


Fig. 1 Model of a canvas painting used in the study

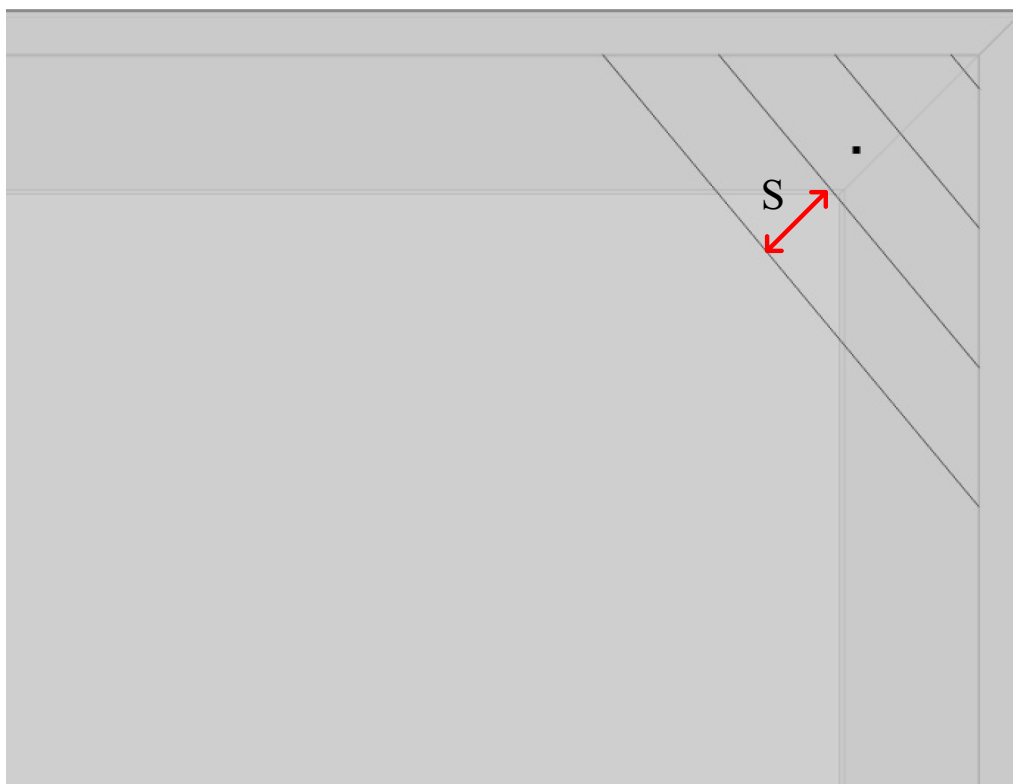


Fig. 2 Location of four cracks separated by distance S . The black dot indicates the point of stress calculation in the mid-thickness of the pictorial layer

The dot in Fig. 2 indicates the point in the middle of the area between the neighbouring cracks at which the stress in the ground layer was calculated. Bai et al. showed that the stress in the direction normal to the developing fracture would reach its maximum in the centre of each area between the cracks for large ratios of crack spacing S to layer thickness t , that is to say, new cracks tend to form approximately in the middle of the uncracked area [26]. It should be borne in mind that the stress field between cracks is not periodic and considering only four cracks has been a necessary simplification due to the limitation of the computational power available to the authors.

In the coordinate system selected, the canvas and ground were stretched in the XY plane, and the Z -axis was oriented perpendicular to the painting's face. The symmetry conditions were applied on the model's internal ZY and ZX boundaries so only one quarter of the painting was modelled. Furthermore, the central point was restrained in the Z -axis translation. These constraints were applied to prevent unwanted movements of the entire model; they did not affect simulations of the painting's response induced by the RH changes.

For uncracked paintings, the swept mesh was used for all components to generate hexahedral elements wherever possible. In the swept meshing process, volume mesh elements are generated by defining a 2D mesh on a surface and propagating it through the modelled domain in discrete steps (for details on mesh sweeping in COMSOL see [27]). Swept meshing allowed the geometry of the painting and solutions of the computed stress fields to be represented with accuracy while controlling the number of elements and minimizing computational resources. Only the angled bars in the corner prevented hexahedrons from forming and triangular prisms were generated in this domain. The total mesh consisted of around 300k elements.

For cracked paintings, swept mesh consisting of triangular prism elements was generally created in a narrow region around the painting's diagonal and in domains between cracks. The number of elements in the region around the diagonal constituted 90–95% of the total mesh. In the remaining areas also tetrahedral elements were generated where required. A statistical analysis of the obtained results was performed for varying dimensions of the narrow region around the diagonal. After finding the optimal mesh, the variability

of solutions fell below 5%, so the results are not presented as a mean and variance of a set of several computations with different meshes but as one solution. The *S/t* ratios are the exception, for which mean values are plotted. The total mesh consisted of around 500k elements for the smallest separation between cracks, and up to 1.4 M elements for the largest separations.

Mechanical properties of chalk-glue ground

The moduli of elasticity of the chalk-glue grounds—the key parameter needed for the modelling—are affected by both the strength of the glue and the ratio of the chalk to the glue. To gain consistent values of the parameter over a broad RH range, a specimen of ground was prepared specifically for this study, and its moduli were measured at RH levels varying between 10 and 90%. The pigment volume concentration (PVC) was 92%. $PVC = P / (P + B)$ where P and B are volumes of the pigment and the dried glue binder, respectively, and the ratio is expressed in percent. Chalk from Champagne from Kremer Pigments Inc. and a 6.7-weight percent water solution of rabbit skin glue from the same producer were used. The historical preparation procedure was adopted after Cennino Cennini [28] as described in [9]. Blocks of the ground were cast into $25 \times 200 \times 150 \text{ mm}^3$ moulds, dried at room conditions for 30 days, and machined to bars of dimensions $6 \times 6 \times 100 \text{ mm}^3$.

The specimens were then glued to cardan joints which helped to reduce the stresses caused by mounting slightly

misaligned specimens, before being tested using a Zwick/Roell Z2.5 TN Universal Testing Machine (UTM) with a 2.5 kN load cell Xforce P grade 1 accuracy. The effective length of the glued specimens was approximately 60 mm. The UTM was placed in an environmental chamber in which the temperature was set to 23 °C and RH was stabilized at the respective RH levels. In the tensile tests, the UTM operated in a displacement control mode at a rate of elongation of 0.125 mm/min corresponding to a strain rate of 0.0042%/s. The displacement was measured using a video-extensometer from Messphysik Materials Testing GmbH of 5 µm accuracy, synchronized with the UTM.

Results

Mechanical properties

Mechanical parameters of the components building up a model painting are detailed in Table 1. The properties of oak white—one of the wood species of moderate stiffness—were assigned to the wooden bars of the stretcher [29]. A parametric study of the influence of the wood’s modulus of elasticity on the stress development in the painting was performed. Stretchers made of stiffer wood than oak white were found to reduce the maximum stresses and render their distributions more uniform. Therefore, medium-hard woods were considered to be the worst-case selection. In the analysis, the moisture-induced dimensional change of wood was neglected as

Table 1 Moduli of elasticity *E*, Poisson’s ratios *ν*, and shear moduli *G* for wood, glue-sized canvas, and chalk-glue ground used in the modelling

Material	Property	Value or formula	Units	Sources
Oak white (<i>L, R, T</i> denote longitudinal, radial, and tangential anatomical directions, respectively)	E_L	12,300	MPa	[29]
	E_R	2005	MPa	
	E_T	886	MPa	
	$G_{LR} = G_{LT} = G_{RT}$	1056	MPa	
	ν_{LR}	0.369	–	
	ν_{LT}	0.428	–	
	ν_{RT}	0.618	–	
Glue-sized canvas (9 × 9 threads/1 cm, 0.63 mm thick)	E_x (warp)	$\frac{160}{1 + e^{(RH - 78.5)/3.5}} + 15$	MPa	[8]
	E_y (weft)	$\frac{410}{1 + e^{(RH - 78.5)/3.5}} + 107$	MPa	
	E_{45} (diagonal)	$\frac{170}{1 + e^{(RH - 78.5)/3.5}} + 3$	MPa	
	E_z	$(E_x + E_y)/2$	MPa	
	ν_{xy}	0.25	–	[8]
	$\nu_{xz} = \nu_{yz}$	0.1	–	Assumed
	$G_{xy} = G_{xz} = G_{yz}$	$\frac{4}{E_{45}} = \frac{1}{E_x} + \frac{1}{E_y} + \left(\frac{1}{G_{xy}} - \frac{2\nu_{xy}}{E_y} \right)$	MPa	[30]
Chalk-glue ground	E_g	$6840 \left[\frac{0.53}{1 + e^{\frac{RH - 24.44}{16.81}}} + \frac{0.47}{1 + e^{\frac{RH - 71.84}{5.99}}} \right]$	MPa	This work
	ν_g	0.2	–	[31]

the stretcher response time to RH variations is much longer than the response time of thin layers of canvas or ground which can be assumed to be instantaneous [8]. Furthermore, under desiccation, the stress in the ground and paint layers is greater when the shrinkage of the stretcher is minimal [18]. Therefore, neglecting it allowed the worst-case scenario to be considered. Finally, this study has focused on cracks induced by the moisture-related dimensional change of glue-sized canvas and the ground layer, and the inclusion of the moisture response of the wooden stretcher would mix the two mechanisms.

Tensile properties of canvases sized with animal glue were adopted from [8]. In the study, the Boltzmann sigmoid function was used to relate their nominal moduli of elasticity to RH determined at a loading of 0.2 kN/m experienced by a well-tensioned canvas painting and using the measured thicknesses of the materials. Despite the large variability of the data determined for various specimens of glue-sized canvases, reflecting the inhomogeneity of glue distribution over the canvas surface, the transition from glassy to ductile state at RH of 78% was satisfactorily described by the Boltzmann function.

Canvas or canvas-glue composites are not homogenous materials. To numerically model the canvas, Mecklenburg and Tumosa established that the mean cross-section area per yarn in the yarns separated from canvases was on average 0.22 of the nominal textile area per yarn, calculated from the measured canvas thickness [32]. The effective thickness of the ‘compact’ fibre layer in the canvases analysed in [8] was accordingly calculated from the measured textile thickness and the number of yarns on the assumption of 0.22 as the ratio between the real and nominal cross-section areas per yarn. In turn the effective thickness of the glue layer in the sized canvases was calculated from the amount of glue and its density. Finally, the effective thickness of the sized canvas was obtained by adding the effective thicknesses of the fibre and glue layers. The parameter was determined to be only 0.21 of the measured material thickness (average for an open-weave canvas CTS2297). The effective moduli were therefore approximately 1/0.21 or 4.7 times larger than the nominal ones given in Table 1.

Moduli of elasticity of the chalk-glue ground determined from the slope of the load-extension curve in the linear region at various RH levels are presented in Fig. 3. The material’s transition from the stiff to ductile (gel-like) state is observed, a tendency well-documented in [33]. Several mathematical functions were tested and the double Boltzmann sigmoid function was fitted to the experimental data as it was found to follow accurately the transition. The parameters obtained from the fit are given in Table 1.

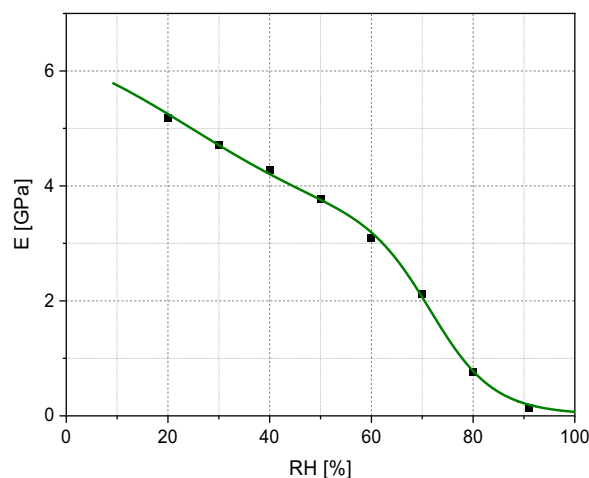


Fig. 3 Elasticity moduli of chalk-glue ground versus RH with the average curve calculated from the fit of the data to the double Boltzmann function

The linear hygroscopic expansion coefficients of the glue-sized canvas and the chalk-glue ground used in the modelling are listed in Table 2. For the canvas, the coefficient perpendicular to the surface was assumed to be an average of the values in the weft and warp directions.

Outcome of the modelling

In the mechanical analysis, stress is expressed as three principal components in mutually perpendicular directions—SP1, SP2, and SP3. SP1 is the maximal stress, SP2 is the maximal stress in directions perpendicular to the SP1, and SP3 is the remaining stress perpendicular to both. In this study, stress was analysed in the middle of the thickness of the ground layer. SP2 was in the out-plane direction and was insignificant. SP1 and SP3 were the in-plane perpendicular components of the stress tensor. The simulations showed that SP1 was positive and SP3 negative, indicating tension and compression, respectively. Figure 4 shows the distribution of SP1 and SP3 induced by a drop in RH from 80 to 30%. The maximum SP1 values arose in the corners of the painting and they decreased towards the centre by a factor of approximately 13 (from 10 to 0.76 MPa). An identical stress decrease factor was obtained for an RH drop from 50 to 10%, that is, in drier conditions. The tensile stress reduction was caused by the shrinkage of the sized canvas, which in turn caused pulling inwards the supporting stretcher (Fig. 5). In consequence, the deformation of the stretcher caused compression in the ground layer instead of tension that would have occurred if the stretcher had been very stiff. The compression was particularly pronounced in the area near the middle parts

Table 2 Linear hygroscopic expansion coefficients β

Material, directions in the canvas		β [10^{-4} per 1% RH]	Sources
Glue-sized canvas (9×9 threads/1 cm, 0.63 mm thick)	x (warp)	3.2	[8]
	y (weft)	0.9	
	z	2.0	Assumed
Chalk-glue ground		0.24	[31]

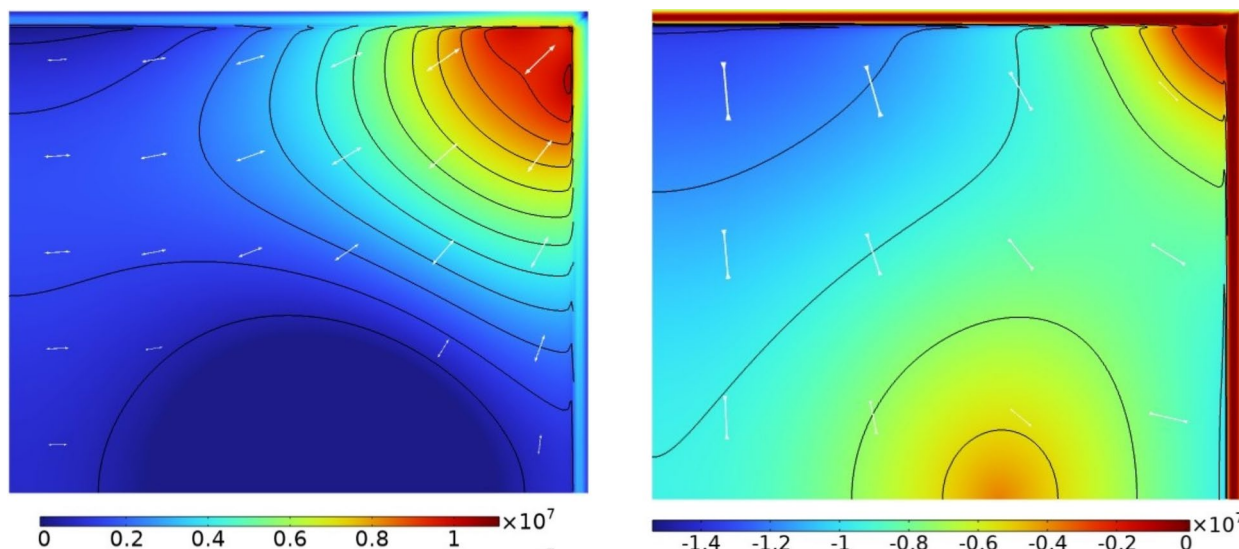


Fig. 4 SP1 (left) and SP3 (right)—engendered in the ground layer by an RH drop from 80 to 30%—shown in a quarter of a painting with the upper right corner. The arrows indicate the directions of the respective stress components

of the stretcher bars where the inward deflection was the largest. The effect weakened closer to the corners as joints of the stretcher bars prevented any significant movement.

The profile of the SP1 plot along the diagonal from the centre to the corner of the painting agrees well with the modelling results obtained by Lee et al. [18] (Fig. 6) while the stress values dramatically differ. The differences in the two studies result from using by Lee et al. mechanical parameters of paint, ground, and glue in the state of full stress relaxation, reflecting stresses in a painting induced by slow variations of environmental parameters, for example, an annual seasonal change in the environment of a painting. Canvas paintings respond in hours to humidity variations and therefore the stress relaxation would be insignificant for short-term variations. The experiments performed with mock-up paintings as well as a small historical painting showed that stress relaxation was much smaller than assumed by Lee et al. [34] and forces induced in the painting by RH variations—measured and modelled—showed a good agreement. This is a crucial issue in the

reliable modelling of paintings as the force produced by the sized canvas and ground layer is the cause of the stretcher deflection.

The simulations showed that varying thickness of the ground layer—from 0.15 mm to 0.3 and 1 mm—had a significant influence on the stress levels as well as the inhomogeneity of the stress distribution but not on the tendencies in the stress distributions. In general, thicker ground layers reduce the overall shrinkage of the sized canvas and in consequence, stresses in the ground are lowered, due to the lower hygric-expansion coefficient of the ground compared to the sized canvas, the deformation of the stretcher decreases, and stress distribution is more uniform.

The plot of SP1 along the diagonal generated by the RH drop from 90 to 20% in the uncracked painting with the 0.15 mm thick ground layer is compared in Fig. 7 with the same plot for the painting in which four cracks were introduced. The maxima in the SP1 between the cracks are located approximately in the middle between cracks and they are larger than the strength of the ground at 20% RH. The strength was calculated as the product of the

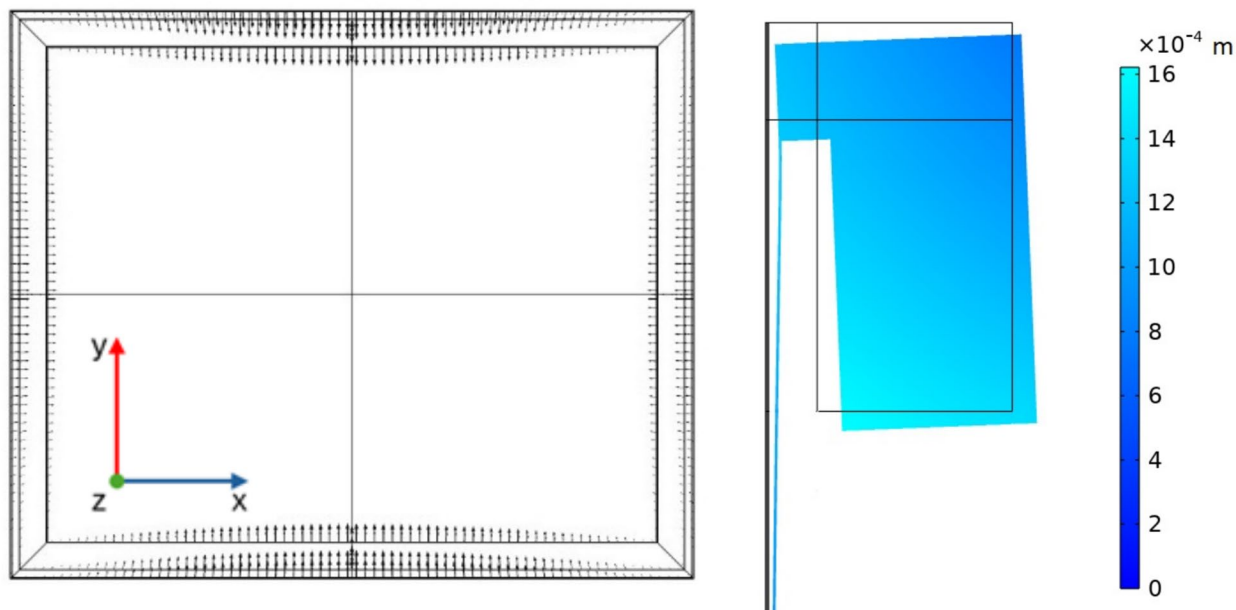


Fig. 5 Planar displacement in the canvas painting engendered by an RH drop from 80 to 30% (the z component of displacement was set to zero) (left); displacement of the top bar in the middle with the initial position indicated by black lines (the deformation is enlarged 2 times for the purpose of visualisation) (right)

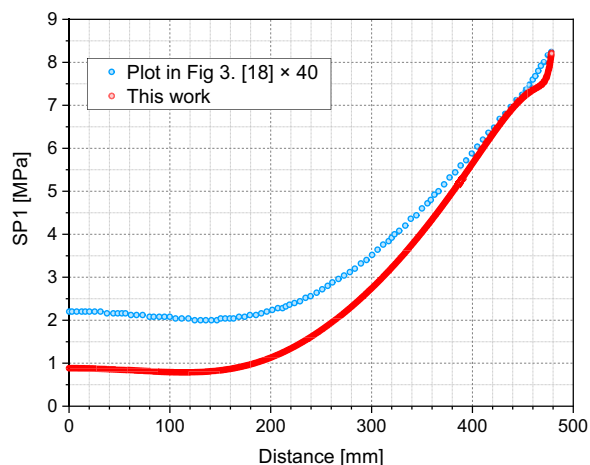


Fig. 6 SP1 along the diagonal from the centre to the corner of the painting obtained in this work and by Lee et al. [18], the latter data are multiplied by a factor of 40

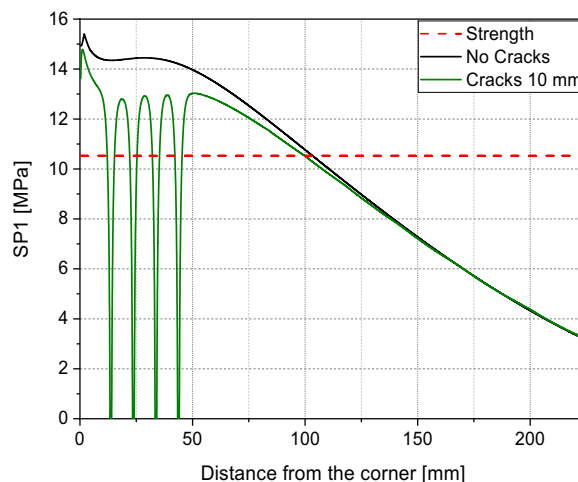


Fig. 7 SP1 induced along the diagonal in a canvas painting by the RH drop from 90 to 20%: no cracks (black line); four cracks separated by a distance of 10 mm (green line). The red dashed line indicates the strength of the ground at 20% RH

modulus of elasticity and the strain at break determined to be around 0.002 at RH below 50% [31].

The relationships between SP1 normalized to the ground layer’s strength σ_0 ($\sigma_0 = E_g(RH) \cdot 0.002$) in the point of stress calculation and the distance between cracks S normalized to the thickness of the ground layer t , termed the S/t ratio, are shown for various RH changes and two thicknesses of the layer in Fig. 8. Using

the normalized stress is a convenient way to relate stress caused by various RH changes to the material’s strength. The normalized SP1 varies slowly for the S/t ratio greater than 50 and drops suddenly for S/t smaller than 25. When the S/t ratio is smaller than 10, SP1 becomes negative, that is stresses become compressive. No new cracks nucleate in the middle of a paint island if normalized

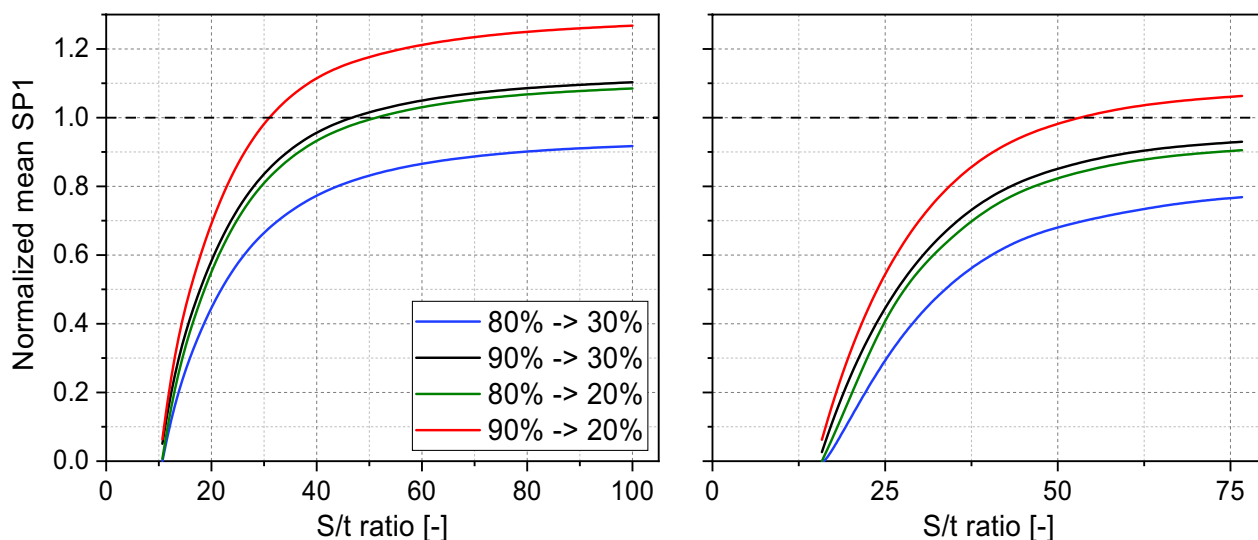


Fig. 8 Normalized mean SP1 engendered in the ground layer of thicknesses 0.15 mm (left) and 0.3 mm (right) by RH drops of varying magnitudes as a function of S/t

SP1 drops below 1. The critical values of S/t defined by these conditions increase for the ground layer thickness of 0.15 mm from 30 to 50 for RH changes of decreasing magnitude. For the thickness of 0.3 mm, the critical value increases to 55 for the largest RH drop considered while smaller RH drops do not induce new cracks at all. The reason for the decreased vulnerability of a canvas painting to RH variations with increasing ground layer thickness is the limitation of the hygric response of the sized canvas by thick ground.

The presence of cracks decreases the vulnerability of the painting to cracking and influences the endangered area in which further cracks may be formed. Natural questions arise as to how many cracks will form, what the distances between them will be, and how the area endangered by further cracking will decrease with the increasing number of cracks formed. Since the calculation of stress fields in a cracked painting is time-consuming and increases with each added crack, methods to provide a quick estimation of crack positions were needed. One such method was to look at the stress just along the diagonal of the painting and compare the stress field in an uncracked painting to stress fields in paintings with an increasing number of cracks. The ratio of SP1 along the diagonal calculated for painting with one crack to the solution without cracks was described by a double Lorentz function with five free parameters:

$$y = y_0 + \frac{2A_1}{\pi} \frac{w_1}{4(x - x_c)^2 + w_1^2} + \frac{2A_2}{\pi} \frac{w_2}{4(x - x_c)^2 + w_2^2} \tag{1}$$

where x_c is the distance from the painting’s corner. The double Lorentz function was chosen out of several

peak functions tested as it followed most precisely the sharp fall and rise of the stress around the crack region. Parameters obtained for the ground layer thickness of 0.15 mm by fitting Eq. 1 to the data were $y_0=1.047$, $A_1=-0.0027$, $A_2=-0.034$, $w_1=0.0017$, $w_2=0.33$. The modelling revealed that the decrease in the magnitude of the SP1 due to the presence of a crack did not significantly depend on the position of the crack. The observation made possible a simple procedure of calculating variations of SP1 along the diagonal on sequential addition of cracks, termed from here the sequential addition procedure, illustrated in Fig. 9. The first crack was located at the point of the highest stress at the distance x_c of 28 mm and the corresponding variation of SP1 was calculated using the function derived. The next crack was located at x_c of 0.014, selected as the least distance of the first crack to the corner in the practical model of a canvas painting developed. SP1 variations along the diagonal were again calculated. The next crack towards the painting’s centre was added at the point of the highest stress at x_c of 0.039. Further cracks can be located towards the painting’s centre using the procedure.

The sequential addition procedure proved very useful in identifying points of the highest stress along the diagonal and locating in them subsequent cracks in the ground layer. As illustrated in Fig. 9, the SP1 variations calculated using the sequential addition procedure agree well with the outcome of the full simulation. However, the procedure is approximate, and performing the full simulation of stress distributions might be needed for the approximate set of cracks established. Figures 10 and 11

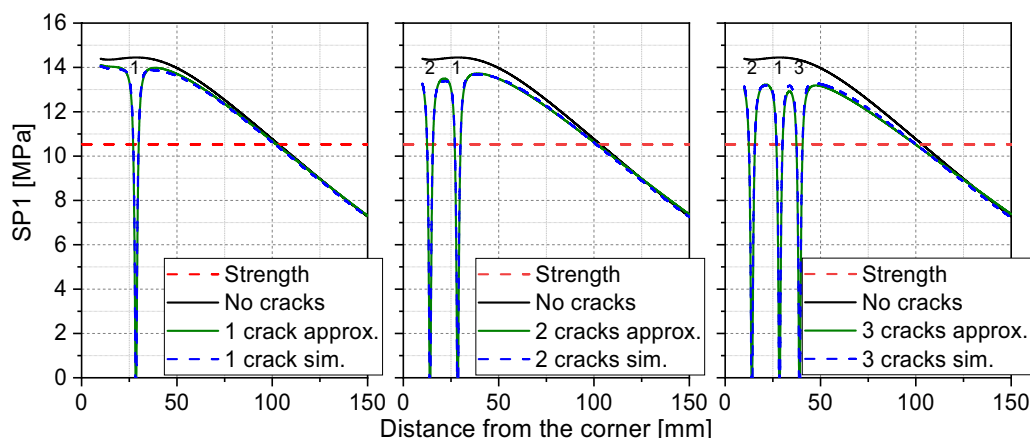


Fig. 9 Plots of SP1 induced along the diagonal in a canvas painting with an increasing number of cracks by the RH drop from 90 to 20%: no cracks (black line), one crack (left), two cracks (middle), and three cracks (right). The red dashed line indicates the strength of the ground at 20% RH. SP1 variations calculated with the use of the sequential addition procedure (solid lines) are compared to the outcome of the full simulation (dashed lines)

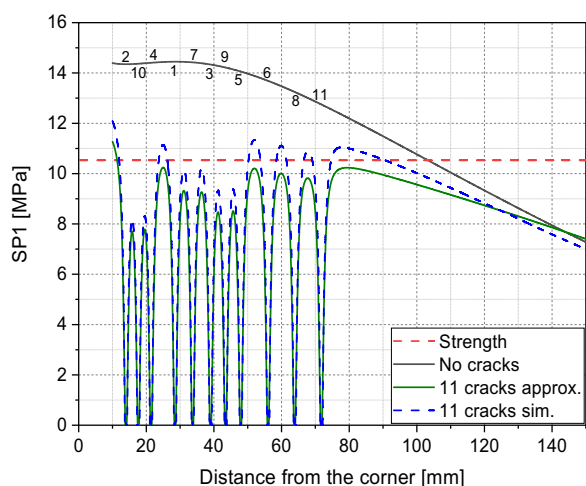


Fig. 10 Plots of SP1 induced along the diagonal in a canvas painting with 11 cracks by the RH drop from 90 to 20%, no cracks (black line). The red dashed line indicates the strength of the ground layer at 20% RH. SP1 variations calculated with the use of the sequential addition procedure (solid lines) are compared to the outcome of the full simulation (dashed lines)

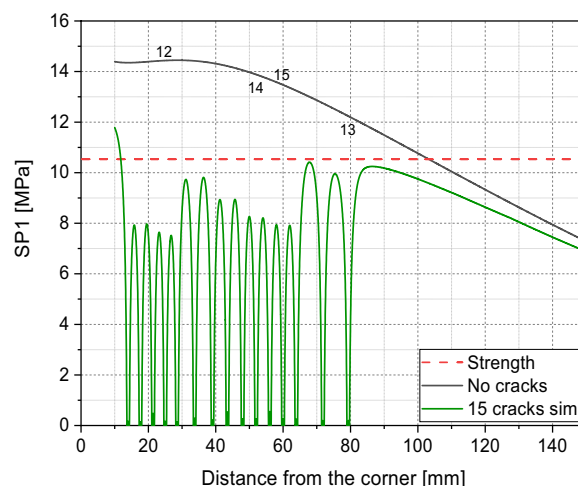


Fig. 11 Plots of SP1 induced along the diagonal in a canvas painting with 15 cracks by the RH drop from 90 to 20%, calculated using the full simulation, no cracks (black line). Additional four cracks were added to 11 cracks illustrated in Fig. 10 at distances of 25, 52, 60, and 79 mm from the corner. The red dashed line indicates the strength of the ground layer at 20% RH

illustrate the issue. The SP1 changes along the diagonal of a painting calculated by locating eleven cracks with the use of the sequential addition procedure are compared with full simulations involving the same cracks in Fig. 10. Although the approximate procedure indicated that the stress in the entire cracked area dropped below the strength of the material and the saturation of the crack patterns occurred, the full simulation indicated stress magnitude exceeding the strength at distances of 25, 52, 60, 68, and 79 mm from the corner. Only when further

four cracks had been introduced at distances of 25, 52, 60, and 79 mm, the stress reduction below the critical level was achieved (Fig. 11).

By way of example, the modelling was applied to the analysis of cracks in a corner of an experimental mock-up painting constructed with a stretched canvas, a hide glue size, and a stiff glue-based ground acting as a design layer and subjected to cycles of large changes in RH (Fig. 43 in [24]). It was reported in the study that additional cycling

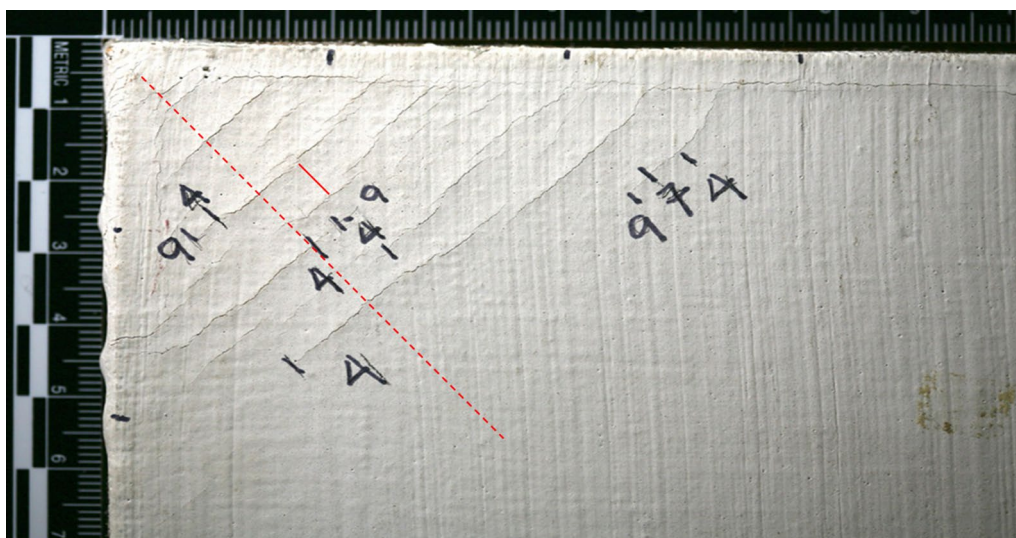


Fig. 12 Mock-up painting with cracks induced by several RH cycles between 95 and 20%. The red line indicates the predicted distance between cracks obtained with the use of the sequential addition procedure and the dashed line indicates the size of the cracked area

beyond the initial nine cycles did no further damage as the cracks that occurred relieved the stresses.

Approximately 9 cracks are visible in the corner shown in Fig. 12 with an average spacing of about 6 mm and a standard deviation of 3 mm. It is expected that the crack spacing should increase with increasing distance from the corner, however, this effect is not evident in this case. It was assumed that the model canvas painting investigated in this study represented adequately the mock-up painting analysed. The sequential addition procedure and the full simulation of 11 or 15 cracks introduced (Figs. 10 and 11) yielded the predicted distance between cracks of 6 ± 2 mm and 5 ± 2 mm, respectively, which agrees very well with the observed one. The predicted cracked area (distances along the diagonal of 72 or 79 mm to the corner) is larger than the observed one but, in general, reflects the overall risk of cracking. There are several sources of uncertainty in the predictions but the most significant lies in the assumption that the stress-free state corresponds to the highest RH level, 90% in the modelling. If the stress-free state in the real painting corresponded to a lower RH level, the model prediction would overestimate the size of the cracked area and underestimate the distance between cracks.

Conclusions

A three-dimensional model for canvas paintings developed in this study comprised a glue-sized canvas on a wooden stretcher with a layer of stiff chalk-glue ground added on the top to represent generally a pictorial layer in historic canvas paintings. The model canvas painting was subjected to a large RH fall of at least 50% RH (from

90 to 20% as a test case study in most simulations) which induced shrinkage of the glue-sized canvas. The modelling demonstrated that when a canvas is stretched on a rigid stretcher providing full restraint to the fabric's movement, a uniform stress field develops due to the restrained shrinkage. If, however, a more realistic stretcher with flexible wooden bars is introduced into the model, high tensile stresses arise in the ground layer at the corners of the painting as the canvas shrinkage causes pulling inwards the supporting stretcher while joints of the stretcher bars prevent any significant movement of the canvas close to the corners.

Owing to the described mechanism, the preferred formation of cracks at the corners of canvas paintings in the direction perpendicular to the diagonal of the painting is frequently observed. The modelling allowed the critical crack spacing normalized to the ground layer thickness, for which stress in the midpoint between the cracks dropped to below the level inducing fracture in the material, to be determined for various magnitudes of the RH drop and thicknesses of the ground layer. Increasing ground layer thickness limits the hygric response of the sized canvas and makes the paintings less vulnerable to RH variations.

The modelling of the response of a canvas painting under desiccation carried out in this and earlier studies has decisively established stress concentration in the painting's corners and the development of corner cracks in the area limited to approximately 5–10% of the diagonal length. Apart from the swelling of the wooden stretchers and the resulting formation of diagonal cracks, it is the only humidity-induced

mechanism of the formation of the ‘ageing’ cracks in this category of paintings. Cracks in the central part of any canvas painting are apparently due to permanent cumulative drying shrinkage of the oil-based paints and grounds restrained by the canvas substrate, due to the evolution of the molecular composition of the oil binder, involving evaporation of low-molecular-weight organic components, and subsequent diffusing out free volume locked in the materials. A recent study of an oil paint layer in a historic painting using X-ray computer microtomography revealed a drying shrinkage of as much as 9% after approximately 400 years of drying which had led to crack systems developed only in the paint layer [6]. The drying shrinkage and the stress field it induces are isotropic and they add to the humidity-induced stress producing complex evolving stress patterns as the paint curing time goes on. Modelling of these stress-building and crack development processes will be the target of future research.

The obtained results indicate that the risk of cracking of the pictorial layers in canvas paintings due to drops in ambient RH is small. In turn, deformation of canvas paintings and risk of physical damage to paint layers at high levels of RH due to the swelling of glue sizing, loss of its adhesive strength, and the resulting delamination of the ground and paints layers from the canvas needs to be further elucidated by modelling and experimental work.

Abbreviations

FEM	Finite element method
PVC	Pigment volume concentration
RH	Relative humidity
UTM	Universal testing machine

Acknowledgements

The authors thank Roman Kozłowski (the Jerzy Haber Institute of Catalysis and Surface Chemistry Polish Academy of Sciences) for his assistance in the interpretation of the results and drafting the manuscript. The authors thank Sergii Antropov (the Jerzy Haber Institute of Catalysis and Surface Chemistry Polish Academy of Sciences) for the help in developing the computer model of a canvas painting.

Author contributions

MB developed and validated the model, performed calculations, analysed and interpreted the data, and prepared the manuscript. LB conceptualized the model, developed the methodology, analysed and interpreted the results, and prepared the manuscript.

Funding

The research leading to these results has received funding from the Norwegian Financial Mechanism 2014–2021, project registration number 2019/34/H/HS2/00581, and the statutory research fund of the Jerzy Haber Institute of Catalysis and Surface Chemistry Polish Academy of Sciences.

Availability of data and materials

Data are available upon request.

Declarations

Competing interests

The authors declare no competing interests.

Received: 11 June 2024 Accepted: 13 October 2024
Published online: 29 October 2024

References

1. Stout GL. Atrial index of laminal disruption. *J Am Inst Conserv.* 1977;17:17–26.
2. Bucklow SL. The description of craquelure patterns. *Stud Conserv.* 1997;42:3129–40.
3. Krzemień L, Łukowski M, Bratasz Ł, Kozłowski R, Mecklenburg MF. Mechanism of craquelure pattern formation on panel paintings. *Stud Conserv.* 2016;61(6):324–30.
4. Poznańska K, Hola A, Kozłowski R, Strojcki M, Bratasz Ł. Mechanical and moisture-related properties of dried tempera paints. *Herit Sci.* 2024;12:25.
5. Pizzimenti S, Bernazzani L, Tinè MR, Treil V, Duce C, Bonaduce I. Oxidation and cross-linking in the curing of air-drying artists' oil paints. *ACS Appl Polym Mater.* 2021;3:1912–22.
6. Janas A, Mecklenburg MF, Fuster-López L, Kozłowski R, Kékicheff P, Favier D, Krarup Andersen C, Scharff M, Bratasz Ł. Shrinkage and mechanical properties of drying oil paints. *Herit Sci.* 2022;10:181.
7. Mecklenburg MF, Tumosa CS, Erhardt D. Structural response of painted wood surfaces to changes in ambient relative humidity. In: Dorge V, Howlett FC, editors. *Painted wood: history and conservation.* Los Angeles: The Getty Conservation Institute; 1998. p. 464–83.
8. Janas A, Fuster-López L, Krarup Andersen C, Escuder AV, Kozłowski R, Poznańska K, Gajda A, Scharff M, Bratasz Ł. Mechanical properties and moisture-related dimensional change of canvas paintings—canvas and glue sizing. *Herit Sci.* 2022;10:160.
9. Bratasz Ł, Akoglu KG, Kékicheff P. Fracture saturation in paintings makes them less vulnerable to environmental variations in museums. *Herit Sci.* 2020;8:11.
10. Jamalabadi MYA, Zabari N, Bratasz Ł. Three-dimensional numerical and experimental study of fracture saturation in panel paintings. *Wood Sci Technol.* 2021;55:1555–76.
11. Antropov S, Bratasz Ł. Development of craquelure patterns in paintings on panels. *Herit Sci.* 2024;12:89.
12. Giorgiutti-Dauphiné F, Pauchard L. Painting cracks: a way to investigate the pictorial matter. *J Appl Phys.* 2016;120:065107.
13. Flores JC. Mean-field crack networks on desiccated films and their applications: girl with a Pearl Earring. *Soft Matter.* 2017;13(7):1352–6.
14. Pauchard L, Giorgiutti-Dauphiné F. Craquelures and pictorial matter. *J Cult Herit.* 2020;46:361–73.
15. Mecklenburg MF. Some aspects of the mechanical behavior of fabric supported paintings. A report to the Smithsonian Institution 1982. In: Rogala DV, DePriest PT, Charola AE, Koestler RJ, editors. *The mechanics of art materials and its future in heritage science, Smithsonian Contributions to Museum Conservation, No. 10.* Washington: Smithsonian Scholarly Press; 2019. p. 107–30.
16. Krarup Andersen C. Lined canvas paintings. Mechanical properties and structural response to fluctuating relative humidity, exemplified by the collection of Danish Golden Age paintings at Statens Museum for Kunst. Thesis. KADK Royal Danish Academy of Fine Arts; 2013.
17. Krarup Andersen C, Mecklenburg MF, Scharff M, Wadum J. With the best intentions. Wax-resin lining of Danish Golden Age paintings (early 19th century) on canvas and changed response to RH. In: Bridgland J, editor. *ICOM Committee for Conservation 14th Triennial Conference, Melbourne, 15–19 September 2014.* Preprints 14.
18. Lee DSH, Kim N, Scharff M, Nielsen AV, Mecklenburg MF, Fuster-López L, Bratasz Ł, Krarup AC. Numerical modelling of mechanical degradation of canvas paintings under desiccation. *Herit Sci.* 2022;10:130.
19. Mecklenburg MF, Tumosa CS. Mechanical behavior of paintings subjected to changes in temperature and relative humidity. In: *Art in transit: studies in the transport of paintings.* Washington D.C: National Gallery of Art; 1991. p. 173–216.
20. Mecklenburg MF, McCormick-Goodhart M, Tumosa CS. Investigation into the deterioration of paintings, and photographs using computerized modeling of stress development. *J Am Inst Conserv.* 1994;33(2):153–70.

21. De Willigen PA. Mathematical study on craquelure and other mechanical damage in paintings. Delft: Delft University Press; 1999.
22. Hendrickx R, Desmarais G, Weder M, Ferreira ESB, Derome D. Moisture uptake and permeability of canvas paintings and their components. *J Cult Herit.* 2015;19:445–53.
23. Stols-Witlox M. A perfect ground. London: Archetype Publications; 2017. p. 50–5.
24. Mecklenburg MF. Determining the acceptable ranges of RH and T in museums and galleries, Part 1. A report of the Museum Conservation Institute, the Smithsonian Institution. 2011. http://www.si.edu/mci/english/learn_more/publications/reports.html. Accessed 17 Mar 2024.
25. Fuster Lopez L. Estudio de la idoneidad de las masillas de relleno en el tratamiento de lagunas en pintura sobre lienzo. Thesis. Universidad Politecnica de Valencia; 2005.
26. Bai T, Pollard DD, Gao H. Explanation for fracture spacing in layered materials. *Nature.* 2000;403:753–6.
27. Fundamentals of swept meshing. [Fundamentals of Swept Meshing \(comsol.com\)](https://www.comsol.com). Accessed 10 Jun 2024.
28. d'Andrea CC. The Craftman's handbook (Il Libro dell'Arte). Translated by Thomson Jr DV. New York: Dover Publications; 1954.
29. Ross RJ. Wood handbook: wood as an engineering material. Centennial ed. General technical report FPL–GTR–190. chap. X. Madison; Department of Agriculture, Forest Service, Forest Products Laboratory; 2010.
30. Penava Ž, Šimić Penava D, Tkalec M. Experimental analysis of the tensile properties of painting canvas. *Autex Res J.* 2016;16(4):182–95.
31. Rachwał B, Bratasz Ł, Krzemień L, Łukomski M, Kozłowski R. Fatigue damage of the gesso layer in panel paintings subjected to changing climate conditions. *Strain.* 2012;48(6):474–81.
32. Mecklenburg MF, Tumosa ChS. An introduction into the mechanical behavior of paintings under rapid loading conditions. In: Mecklenburg MF, editor. *Art in transit: studies in the transport of paintings*. Washington: National Gallery of Art; 1991. p. 137–71.
33. Bridarolli A, Freeman AA, Fujisawa N, Łukomski L. Mechanical properties of mammalian and fish glues over range of temperature and humidity. *J Cult Herit.* 2022;53:226–35.
34. Bury M, Janas A, Bratasz Ł. Unpublished study. The Jerzy Haber Institute of Catalysis and Surface Chemistry. Krakow: Polish Academy of Sciences; 2023.

Publisher's Note

Springer Nature remains neutral with regard to jurisdictional claims in published maps and institutional affiliations.